Paper No. 422 4th International Conference on Multiphase Flow, ICMF-2001
New Orleans, U.S.A., May 27-June 1, 2001

NUMERICAL STUDY OF PARTICLE-LADEN ROTATING TURBULENCE

Yingkang Pan, Toshitsugu Tanaka and Yutaka Tsuji
Department of Mechanophysics Engineering, Osaka University, Suita 565-0871, JAPAN

Abstract

Dynamics of turbulence modulation and particle concentration in rotating flows, at a low particle volume fraction $O(10^{-5})$, is studied using direct numerical simulation (DNS). Simulation results demonstrate that particle clusters parallel to the rotating axis are observed when the rotation effect is strong. No special particle concentration is observed in the decaying turbulence of the stationary case. It is also found that particles enhance the degree of turbulence decaying at the beginning of time, and they increase the turbulence intensity after a very short period of time. From the present DNS, it is found that the turbulence modulation due to the existence of particles can be judged by observing the ratio of the rotation time scale $(1/2\Omega)$ to the particle momentum time scale τ_p. From simulated results it also can be seen that the inter-particle collision rate decreases very quickly for the stationary case, and it increases by increasing the rotating angular velocity. It is obtained that both rotation and particles have an anisotropic effect on the fluid turbulence.

1. Introduction

The particle-turbulence interaction has become one of the most interesting topics in multiphase flow because of new interesting phenomena existed and the many practical applications. Especially in a rotating system, the motion of particles is much affected by the Coriolis forces besides other forces, so that particle's behaviors considerably deviate from that of the carrier fluid. Particle transport in the rotating turbulent flows is little known because of its complication. On the other hand, turbulence modification by particles occurs when the particle volume fraction reaches as $O(10^{-5})$, such that the momentum loss or gain to the turbulence by the particles is no longer negligible. Direct numerical simulations including particle feedback (or called two-way coupling) on fluid-phase turbulence appeared in the past decade. Squires and Eaton (1990) firstly studied the turbulence modification by particles using direct numerical simulations of isotropic turbulence. Elghobashi and Truesdell (1993) investigated the effects of particle response time, particle diameter, particle volume fraction and gravity on turbulence structure in decaying homogeneous turbulence using direct numerical simulations. Recently, Boivin *et al.* (1998) performed the DNS of isotropic turbulence to study the turbulence modulation by dispersed particles. They found that particles increasing dissipate fluid kinetic energy with increasing loading, with the reduction in kinetic energy being relatively independent of the particle relaxation time. They also discovered that viscous dissipation in the fluid decreases with increasing loading and is larger for particles with smaller relaxation times. Sundaram and Collins (1999) performed the DNS of isotropic turbulence by suspended particles considering the particle interactions with a hard-sphere model. They extended their formalism to compute two-point energy correlations and spectra of the particle-laden flow field. They also observed that the particle inertia increases both the viscous and drag dissipations, and causes particle velocities to correlate for longer distance.

Although particle-laden rotating turbulence in a cube with periodic boundary conditions in three directions is an anisotropic turbulence due to both the particles and the Coriolis forces, the analytical method for isotropic turbulence is still powerful and is employed to study the turbulence modulation and particle concentration in the present simulations.

2. Mathematical description

Figure 1 illustrates the coordinate system used to write the equations of motion. Incompressible turbulence subjected to uniform solid-body rotation at angular rotating velocity Ω about the *z*-axis in a Cartesian coordinate system, having no mean flow, is considered for simplicity. The fluid phase in a rotating cube is governed by the incompressible continuity and Navier-Stokes equations. The influence of particles on the continuity equation of the fluid is assumed negligible because of very low particle volume fraction $O(10^{-5})$ in the present simulations. So the final governing equations in a relative coordinate system (*x*, *y*, *z*) can be expressed in the following forms

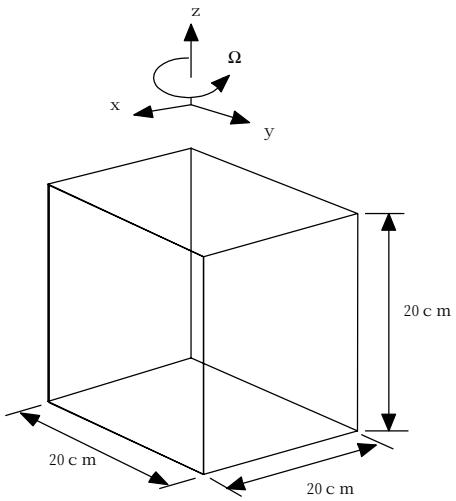

Fig. 1 Flow geometry and coordinate system

$$\frac{\partial u_j}{\partial x_j} = 0, \tag{1}$$

$$\frac{\partial u_i}{\partial t} + \frac{\partial}{\partial x_j}\left(u_i u_j\right) = -\frac{\partial p_{eff}}{\partial x_i} + \nu \frac{\partial^2 u_i}{\partial x_j \partial x_j} + 2\varepsilon_{ij3}\Omega u_j + F_{p,i}, \tag{2}$$

where δ_{ij} is the Kronecker delta symbol, ε_{ijk} the Levi-Civita's alternating tensor. The third term in the right hand side in Eq. (2) is the Coriolis force experienced by a fluid element resulting from system rotation. The effect of gravity on the fluid is assumed negligible. The centrifugal force is conservative in nature. $F_{p,i}$ in Eq. (2) is the reaction of fluid force on particles contains in a unit mass of fluid element. If we do the one-way coupling simulation, $F_{n,i}$ is set to be zero. Periodic boundary conditions in all three directions are applied here for simplicity.

If all particles are rigid spheres with identical diameter d_p and density ρ_p, and the density of the particles is much larger than that of the carrier fluid, the equation of particle motion can be simplified in a rotating frame of reference with the axis of rotation aligned with *z* direction. It can be given in the following dimensional form

$$m_p \frac{du_{pi}}{dt} = \frac{1}{2}\rho\left|\mathbf{u}_R\right| A\left[C_D u_{Ri} + C_{LR}\frac{\left(\mathbf{u}_R \times \boldsymbol{\omega}_R\right)_i}{\left|\boldsymbol{\omega}_R\right|}\right] + 2\varepsilon_{ij3} m_p \Omega u_{pj}. \tag{3}$$

The last term in Eq. (3) is the Coriolis force. For isolating the effects of the Coriolis force, body forces (gravity and centrifugal force) were not considered here. The rotating cube can be regarded in the location very far from the axis, and the mean flow is removed due to the body forces. Because of having no mean flow, the saffman lift force is so small that it can be neglected in the present simulations (Saffman, 1965). The empirical relation for C_D (Schiller and Nauman, 1933) was employed, as

$$C_D = \frac{24}{Re_p}\left(1 + 0.15 Re_p^{0.687}\right). \tag{4}$$

In the present simulations we employed the Rubinow-Keller lift coefficient C_{LR} for Re_p<1 and the lift coefficient C_{LR} for Re_p>1 according to Oesterle and Dinh (1998). It can be expressed as

$$C_{LR} = \begin{cases} 2.0\gamma \quad \text{for} \quad Re_p \le 1.0, \\ 0.45 + (2\gamma - 0.45)\exp(-0.075\gamma^{0.4}\ \mathrm{Re}_p^{0.7}) \text{for } Re_p > 1.0, \end{cases} \tag{5}$$

where γ is the dimensionless angular velocity of a particle, $\gamma = d_p \left|\boldsymbol{\omega}_R\right| / \left|\mathbf{u}_R\right|$. The equation of rotational motion of a particle is given by

$$I \frac{d\omega_{pi}}{dt} = -C_T \frac{1}{2}\rho\left(\frac{d_p}{2}\right)^2 \left|\boldsymbol{\omega}_R\right| \omega_{Ri}, \tag{6}$$

where I is the moment of inertia of a particle. The right hand side of Equation (6) is the viscous torque against the particle's rotation, which is theoretically obtained by Dennis *et al.* (1980) and Takagi (1977). C_T is the non-dimensional coefficient determined by the rotational Reynolds number, $Re_R = d_p^2 \left|\boldsymbol{\omega}_R\right| / 4\nu$.

Inter-particle collisions take an important role in the turbulence production and dissipation in the rotating flows due to high local particle concentrations. In the present situations, particle number density is so low, so that we applied the deterministic method (Tanaka and Tsuji, 1991). Collision is mainly detected by calculating the distance of two particle's centers at the specific time when two particles collide with each other.

The governing equations (1) and (2) were solved numerically using a semi-implicit method. The divergence form (2) we used is conservative for finite-difference schemes when a staggered grid is applied. Spatial derivatives were approximated by second-order accuracy central difference scheme. The advancement scheme for the velocity components u_i is a compact-storage third-order Runge-Kutta scheme published by Spalart *et al.* (1991) which has an explicit treatment for the convective terms and the source terms including the particle feedback, and second-order-implicit Crank-Nicolson for the viscous term. An approximate factorization technique in three directions combined with fractional step procedure (Kim and Moin, 1985) is used to get the prediction values of velocities. The Poisson equation for pressure can be solved using Fourier series expansions in all three directions because of the periodic boundary conditions in those directions.

The velocity or the rotation velocity of a particle can be obtained by integrating Equation (3) or (6) using the second-order Adams-Bashforth explicit scheme, the position of a particle can be got according to the velocity. Because only the velocity of the flow field at every grid point was known, so the 3-D 8-node Lagrangian interpolation polynomial was used to obtain the velocities of the carrier fluid at the positions of the particles.

3. Results

In the numerical experiments the calculation cube used was 20 *cm* in each direction. The calculation domain was divided into 64^3 computational cells with a uniformly spaced grid

in each direction. To obtain the initial turbulence intensity to be 0.9586 *m/s* and initial Marco-scale Reynolds number, Re_λ, to be 91.35, the fluid is assumed with the properties ($\nu = 6.0\times10^{-5}\ m^2/s$, $\rho = 1.2\ kg/m^3$) in the present simulations. The assumed kinematic viscosity of fluid is four times of that of normal air. Initial turbulence having no mean flow was generated at random. 262144 particles with the diameter d_p=100 μm and the density $\rho_p = 1800\ kg/m^3$, were initially placed at random, non-contact positions and assigned fluid velocity to begin with. According to the particle volume fraction $\phi_v = 1.716\times10^{-5}$, the two-phase flow is still located in the region of the "dilute" case. Considering the inter-particle collisions, both the fluid and the dispersed particles are simulated in dimensionalized units. The time steps used were 0.001 second for the fluid and the particle motion and 0.003 second for the inter-particle collisions. After applying the hard-sphere model for inter-particle collision we set the coefficient of restitution e_p equal to 0.95 and the coefficient of friction μ_p equal to 0.3 for all cases. 4000 time steps (total 4 seconds) were carried out for one stationary case (Ω=0 s^{-1}) and two other cases with different angular velocities (Ω=20 and 80 s^{-1}). Based on above assumptions, the initial turbulence can be regarded as a nearly isotropic turbulence. Therefore, some traditional techniques for isotropic turbulence may be employed to observe the turbulence modulation in particle-laden rotating turbulence. Similarly, according to the Navier-Stokes equations (2) the transport equations for the fluid turbulence kinetic energy $K = \frac{1}{2}u_i u_i$ and dissipation rate $\varepsilon \equiv \nu\left(\partial u_i/\partial x_j\right)^2$ can be given by

$$\frac{dK}{dt} = \dot{F} - \varepsilon, \tag{7}$$

$$\frac{d\varepsilon}{dt} = P_e - D_e - F_e, \tag{8}$$

where

$$\dot{F} \equiv u_i F_{p,i}, \qquad P_e \equiv -2\nu \frac{\partial u_i}{\partial x_j}\cdot\frac{\partial u_i}{\partial x_k}\cdot\frac{\partial u_j}{\partial x_k},$$

$$D_e \equiv 2\nu^2 \frac{\partial^2 u_i}{\partial x_j \partial x_k}\cdot\frac{\partial^2 u_i}{\partial x_j \partial x_k}, \qquad F_e \equiv 2\nu \frac{\partial u_i}{\partial x_j}\cdot\frac{\partial F_{p,i}}{\partial x_j}.$$

$\dot{F}$ is the fluid-particle energy exchange rate. P_e, D_e and F_e in Eq. (8) are the production by turbulent vortex stretching, viscous destruction of dissipation and fluid-particle dissipation exchange rate, respectively.

Figures 2 and 3 show the evolutions of the fluid-particle exchange rates of energy and dissipation for various values of Ω. The exchange rates of energy and dissipation can be neglected for the stationary case, and the case with smaller angular velocity Ω=20 s^{-1}. For the case with a higher angular velocity Ω=80 s^{-1}, at the beginning of time, particles enhance the degree of turbulence decaying. On the other hand, they increase the turbulence intensity after a very short period of time. Moreover, large peaks of $\dot{F}$ and F_e can be observed both for *t* about 1.8 *s*, and minimum values for *t* about 2.0 *s*. It also can be seen that the fluid-particle exchange rates of kinetic energy and dissipation are different with time and their values are not smooth with time because of the inter-particle collisions. Accordingly, there exist maximum values of turbulence and integral length scales at $t = 1.8\ s$ where its macro-scale Reynolds number reaches the maximum for the case with Ω=80 s^{-1}.

A conventional nondimensional measure of the strength of rotation is given by comparing the rotation time scale (1/2Ω) to the turbulence time scale, giving the turbulent

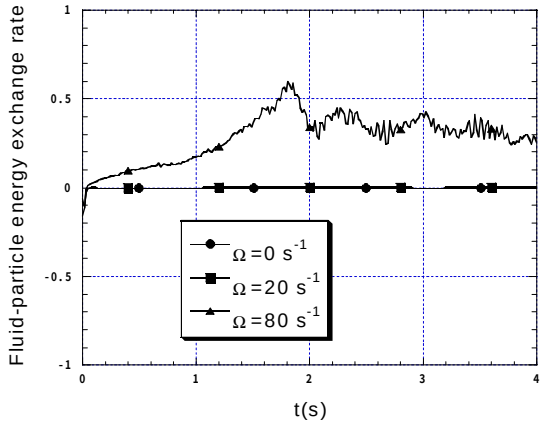

Fig.2 Evolution of fluid-particle energy exchange rate with time, $\dot{F}$. The dimensional unit of $\dot{F}$ is m^2/s^3 .

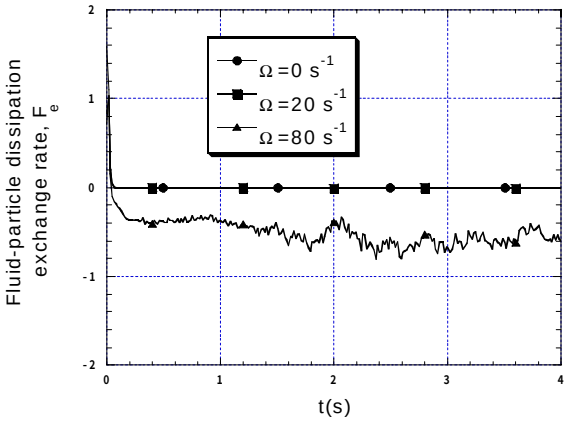

Fig.3 Evolution of fluid-particle dissipation exchange rate with time, F_e. The dimensional unit of F_e is m^2/s^4 .

Rossby number $Ro_T \equiv \varepsilon/(2K\Omega)$. A comparison with other time scales representing large-scale and small-small scale motions may also be useful, leading to macro- and micro-Rossby numbers (Cambon *et al.*, 1997), respectively. Similarly, in the rotating system we can observe the ratio of the rotation time scale (1/2Ω) to the momentum response time τ_p or the particle mean free time τ_c

$$Ro_p \equiv 1/(2\Omega\tau_p); \qquad Ro_c \equiv 1/(2\Omega\tau_c). \tag{9}$$

These ratios may provide a convenient measure of the importance of Coriolis forces in a rotating system. In the present simulations, the momentum response time of the particle keeps constant 0.01389 *s* as the particle Reynolds number is always smaller than 1. For the case with Ω=20 s^{-1} the rotation time scale is $1.8\tau_p$, and for the case with Ω=80 s^{-1} it is $0.45\tau_p$. From above, it can be obtained that the fluid-particle exchange rates of kinetic energy and dissipation can be obviously detected at (1/2Ω)<τ_p. From the simulations it also can be seen that the rotation time scale is much smaller than the mean free time of particles. So the inter-particle collisions play an important role for the case with Ω=20 or 80 s^{-1}.

A quantitative comparison of the particle concentrations can by made by introducing the root mean square values of particle number per cell over the whole field (Ling *et al.*, 1998),

$$N_{rms} = \left(\sum_{j=1}^{N_{cp}} N_j^2 \Big/ N_{cp} \right)^{1/2}, \tag{10}$$

where N_{cp} is the total number of computational cells and N_j is the number of particles in the *jth* cell. Figure 4 shows the dynamics of N_{rms} for different angular velocities with time. No special particle concentration has been detected for the stationary case in which N_{rms} almost keeps constant of 1.45. On the other hand, particles gradually accumulate in low-vorticity, high strain-rate regions with time at a smaller angular velocity Ω=20 s^{-1}. For the case with Ω=20 s^{-1}, N_{rms} has a peak value about 3.3 at time about 2.4 *s*. Particle concentration is easily observed at an earlier time. In order to study the detailed pattern of the particle concentration, a 3-D isosurfaces of particle number per cell is used to demonstrate the patterns of the particle concentrations (Fig. 5). No special structures have been observed for the stationary case. For the other two cases with Ω=20 and 80 s^{-1}, special particle clusters parallel to the rotating axis (*z*) have been observed.

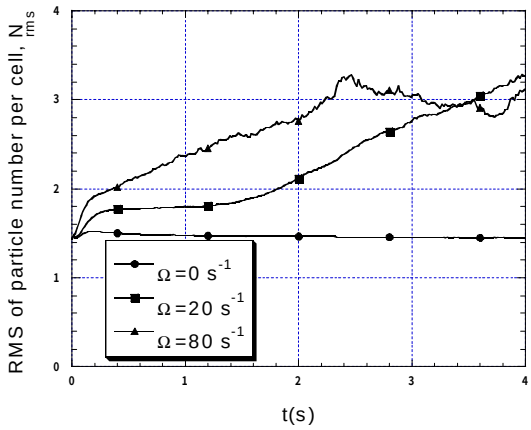

Fig. 4 Root-mean-square values of particle number per cell with time.

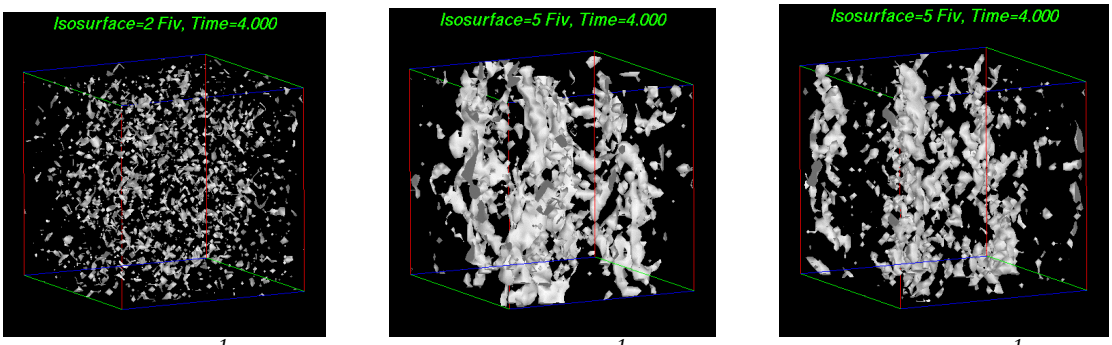

(a) Ω=0 s^{-1} (b) Ω=20 s^{-1} (c) Ω=80 s^{-1}

Fig. 5 Isosurfaces of particle number per cell at time t=4 s

The effect of rotation on the inter-particle collision rate can be obviously obtained through Fig. 6. The inter-particle collision rate drastically decays with time for the stationary case. On the other hand, the inter-particle collisions enhances by increasing the rotating angular velocity Ω. When the rotating angular velocity becomes higher, the inter-particle collision rate is unstable with time. For the case with Ω=80 s^{-1}, the inter-particle collision rate has some peaks corresponding to the maximum or minimum fluid-particle exchange rates of kinetic energy and dissipation. Because of the strong rotation of the cases with Ω=20 and 80 s^{-1}, the calculated inter-particle collision rate with a hard-sphere model is much higher than that predicted by Abrahamson (1975) or Saffman and Turner (1956) with time according to Fig. 6.

By observing the one-dimensional energy spectra in three directions, it is demonstrated that the particles enhance the fluid turbulence energy at high wavenumbers greater than 60 for the stationary case. For the case with Ω=80 s^{-1} the particles enhance the fluid turbulence in whole regions from low to high wavenumbers.

However, the turbulence modulation by particles in the present simulations can be obtained by observing the dynamics of one-point and two-point velocity correlations. The fluid-particle cross terms of one-point velocity correlations, $R_{ij}^{fp} \equiv \langle u_i u_{p,j} \rangle$, are often regarded as zero for the stationary particle-laden isotropic turbulence (Sundaram and Collins, 1997). From the present simulations, it is demonstrated that the terms of R_{ij}^{fp} are negligibly small for the stationary and weak rotation (Ω=20 s^{-1}) cases. On the contrary, those terms of R_{ij}^{fp} are no longer negligibly small for the strong rotation case (Ω=80 s^{-1}) from Fig.7, especially the terms, R_{ii}^{fp}, R_{12}^{fp} and R_{21}^{fp}, in which the rotating axis is parallel to z (x_3) direction.

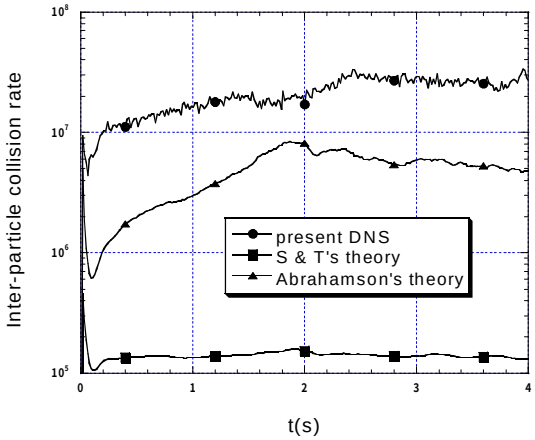

Fig.6 Comparison of the inter-particle collision rates among from the present DNS, Suffman and Turner's theory and Abrahamson's theory with time for the case with Ω=80 s^{-1}.

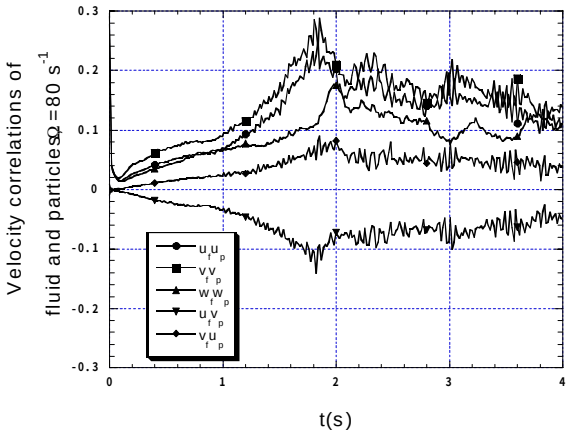

Fig.7 Time development of one-point velocity correlations between the fluid and the particles for the case with Ω=80 s^{-1}.

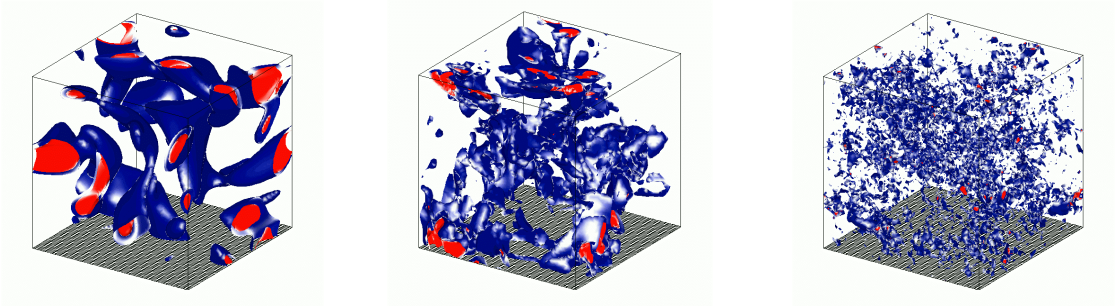

(a) Ω=0 s^{-1} (b) Ω=20 s^{-1} (c) Ω=80 s^{-1}

Fig. 8 Isovorticity surfaces of different cases at time t=4 s.

The terms, R_{ii}^{fp}, R_{12}^{fp} and R_{21}^{fp}, have peaks near t=1.8 s where the fluid-particle exchange rates reach their maxima. Moreover, the magnitudes of R_{ii}^{fp} are larger than that of R_{12}^{fp} or R_{21}^{fp} corresponding to the same time. The term of R_{12}^{fp} has an opposite value compared to R_{21}^{fp}.

The isovorticity surfaces at different rotating angular velocities at time t=4 s are shown in Fig. 8. Weak and strong rotations have different vortex structures. The vortex is broken into small scales at a higher rotating angular velocity Ω=80 s^{-1} although the absolute values are much larger than that of other cases.

4. Conclusions

The results show that particles concentrate in low-vorticity, high strain-rate regions when the rotation effect is strong, furthermore, the particles clusters parallel to the rotating axis can be observed. No special particle concentration is observed in decaying turbulence without system rotation.

From the present DNS, it is found that the turbulence modulation due to the existence of particles can be judged by observing the ratio of the rotation time scale $(1/2\Omega)$ to the particle momentum time scale τ_p. It is also found that particles enhance the degree of turbulence decaying at beginning of time, on the other hand, they increase the turbulence intensity after a very short period of time. From simulated results it also can be seen that the

inter-particle collision rate decreases very quickly for the case without rotation, and it is increasing by increasing the rotating angular velocity Ω. When the rotating angular velocity becomes higher, the inter-particle collision rate is unstable as time goes on.

Numerical results also show that both rotation and particles have an anisotropic effect on the fluid turbulence. The fluid-particle cross terms of one-point velocity correlations cannot be neglected when the rotation time scale $(1/2\Omega)$ is less than the momentum particle response time τ_p.

5. References

J. Abrahamson, Collision Rates of Small Particles in a Vigorously Turbulent Fluid, *Chem. Eng. Sci.*, vol. 30, pp. 1371-1379, 1975.

M. Boivin, O. Simonin and K.D. Squires, K., 1998. Direct numerical simulation of turbulence modulation by particles in isotropic turbulence. *J. Fluid Mech.*, vol. 375, pp. 235-263, 1998.

C. Cambon, N.N. Mansour and F.S. Godeferd, Energy Transfer in Rotating Turbulence, *J. Fluid Mech*., vol. 337, pp. 303-332, 1997.

S.C.R Dennis, S.N. Singh and D.B. Ingham, The Steady Flow Due to a Rotating Sphere at Low and Moderate Reynolds Number, *J. Fluid Mech.*, vol. 101**,** pp. 257-279, 1980.

S. Elghobashi and G.C. Truesdell, On the Two-Way Interaction Between Homogeneous Turbulence and Dispersed Solid Particles. I: Turbulence Modification, *Phys. Fluids* A, vol. 5 (7), pp. 1790-1802, 1993.

J. Kim and P. Moin, Application of a Fractional-Step Method to Incompressible Navier-Stokes Equations, *J. Comput. Phys.*, vol. 59, pp. 308-323, 1985.

W. Ling, J.N. Chung, T.R. Troutt and C.T. Crowe, Direct Numerical Simulation of a Three-Dimensional Temporal Mixing Layer with Particle Dispersion, *J. Fluid Mech.*, vol. 358**,** pp. 61-85, 1998.

B. Oesterle and T.B. Dinh, Experiments on the Lift of a Spinning Sphere in a Range of Intermediate Reynolds Numbers, *Experiments in Fluids*, vol. 25, pp. 16-22, 1998.

S.I. Rubinow and J.B. Keller, The Transverse Force on a Spinning Sphere Moving in a Viscous Fluid, *J. Fluid Mech.*, vol. 11, pp. 447-459, 1961.

P.G. Saffman, The lift on a Small Sphere in a Slow Shear Flow, *J. Fluid Mech.*, vol. 22(2), pp. 385-400, 1965.

P.G. Saffman and J.S. Turner, On the Collision of Drops in Turbulent Clouds, *J. Fluid Mech.*, vol. 1, pp. 16-30, 1956.

L. Schiller and A. Nauman, A., V. D. I. *Zeits.*, vol. 77, pp. 318, 1933.

P.R. Spalart, R.D. Moser and M.M. Rogers, Spectral Methods for the Navier-Stokes Equations with One Infinite and Two Periodic Directions, *J. Comput. Phys.*, vol. 96, pp. 297-324, 1991.

K.D. Squires and J.K. Eaton, Particle Response and Turbulence Modification in Isotropic Turbulence, *Phys. Fluids* A, vol. 2 (7), pp. 1191-1203, 1990.

S. Sundaram and L.R. Collins, A Numerical Study of the Modulation of Isotropic Turbulence by Suspended Particles, *J. Fluid Mech.*, vol. 379, pp. 105-143, 1999.

H. Takagi, Viscous Flow Induced by Slow Rotation of a Sphere, *J. Phys. Soc. Japan*, vol. 42, pp. 319-325, 1977.

T. Tanaka and Y. Tsuji, Y., Numerical Simulation of Gas-Solid Two-Phase Flow in a Vertical Pipe: on the Effect of Inter-Particle Collision, *ASME/FED Gas-Solid Flows*, pp.123-128, 1991.